Cogn Neurodyn (2008) 2:115–120
DOI 10.1007/s11571-008-9044-2

RESEARCH ARTICLE

Cortical network dynamics with time delays reveals functional connectivity in the resting brain

A. Ghosh · Y. Rho · A. R. McIntosh · R. Kötter · V. K. Jirsa

Received: 14 January 2008 / Accepted: 30 March 2008 / Published online: 23 April 2008

Abstract In absence of all goal-directed behavior, a characteristic network of cortical regions involving prefrontal and cingulate cortices consistently shows temporally coherent fluctuations. The origin of these fluctuations is unknown, but has been hypothesized to be of stochastic nature. In the present paper we test the hypothesis that time delays in the network dynamics play a crucial role in the generation of these fluctuations. By tuning the propagation velocity in a network based on primate connectivity, we scale the time delays and demonstrate the emergence of the resting state networks for biophysically realistic parameters.

Keywords Resting brain · Default mode

Introduction

The primate brain exhibits spontaneous coherent fluctuations in absence of all environmental stimuli and goal directed behavior (Biswal et al. 1995; Gusnard and Raichle 2001; Fox et al. 2005; Greicius et al. 2003; Damoiseaux et al. 2006; Vincent et al. 2006; Bar 2007). These fluctuations primarily occur in a network consisting of prefrontal, parietal and cingulate cortices. In humans, this network has been shown to greatly overlap with functional architectures present during consciously directed activity and hence various functional roles such as "day-dreaming" or "stimulus-independent thought" have been attributed to it. Just recently it has been put forward that the transient resting state activations are reminiscent of features of a more fundamental organization of the cortex. This proposal has been motivated by the identification of the presence of similar resting state networks in monkeys during deep anaesthesia (Vincent et al. 2007). In the present paper, we put this hypothesis to test and investigate if a neural network dynamics with realistic primate connectivity and time delays is capable of generating the coherent rest state fluctuations. The introduction of time delays is well motivated, since we deal with large-scale connectivity (Jirsa 2004) involving far distant brain areas.

Anatomical connectivity analysis

The basis of our network is the connectivity matrix of one hemisphere obtained from the CoCoMac database (Kötter 2004). This primate anatomical connectivity matrix (collated from macaque tracing studies) comprises 38 nodes with weights ranging from 0 to 3. The corresponding "Regional map" gives the translation between macaque and human neuroanatomy (Kötter 2005). To quantify the connectivity characteristics, we computed a set of network connectivity measures (Honey et al. 2007) for all nodes including the in- and out-degree of connectivity and the

A. Ghosh (✉) · V. K. Jirsa
Theoretical Neuroscience Group, UMR6152 Institut de Science du Mouvement CNRS, 163 Avenue de Luminy, CP 910, 13288 Marseille Cedex 9, France
e-mail: Anandamohan.GHOSH@univmed.fr

Y. Rho · V. K. Jirsa
Center for Complex Systems & Brain Sciences, Physics Department, Florida Atlantic University, 777 Glades Road, Boca Raton, FL 33431, USA

A. R. McIntosh
Rotman Research Institute, Baycrest, 3560 Bathurst Street, Toronto, ON, Canada M6A 2E1

R. Kötter
Donders Centre for Neuroscience, Department of Cognitive Neuroscience, Radboud University, Geert Grooteplein 21, Nijmegen 6525 EZ, The Netherlands

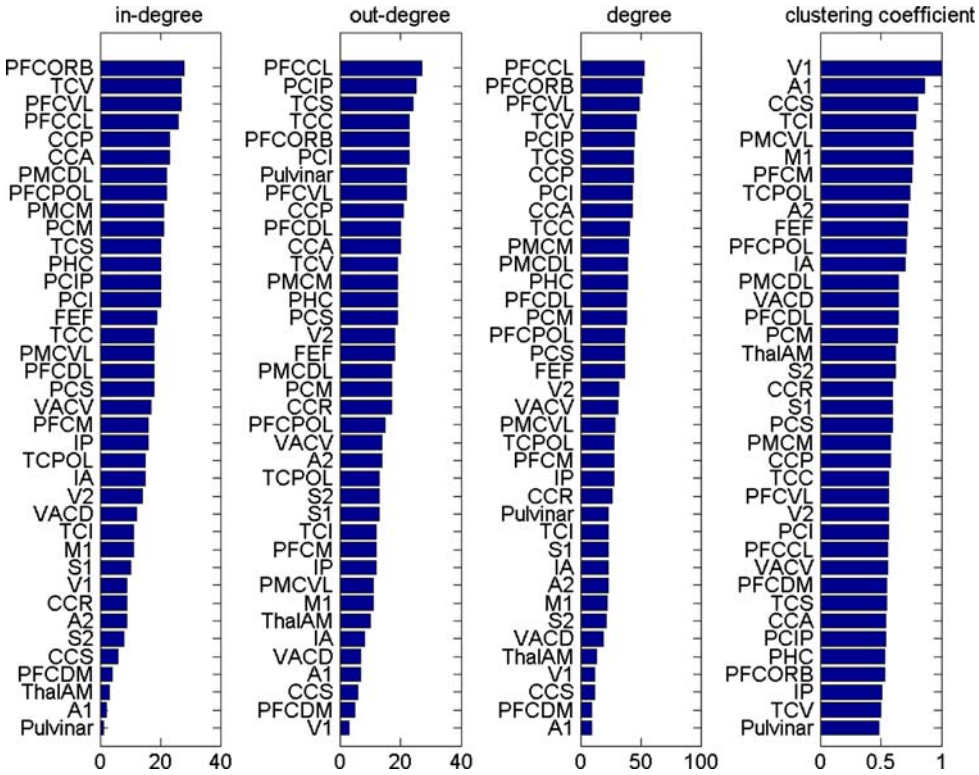

Fig. 1 Characterization of the primate connectivity matrix: node wise degree distributions and clustering index

clustering coefficient (see Fig. 1). The in-degree and out-degree are computed as the number of incoming and outgoing connections to/from a node, respectively, giving a measure of how much information it can receive or give. The degree is the sum of in- and out-degree. The clustering coefficient is calculated as the number of all existing connections between a node's neighbors divided by all such possible connections. The connection graph has 599 edges, with connection density = 0.426, characteristic path length = 1.633 and clustering index = 0.568.

Our analysis shows that the components of the rest state network are not clearly differentiated from other network nodes. Anatomically the prefrontal cortex is characterized by a large degree of afferent and efferent connectivity, whereas cingulate and parietal areas display only a moderate degree of connectivity. Clustering index is commonly used to identify hubs in a network, but does not differentiate the default network either. Previous anatomical analyses evaluating whether the correlation between spontaneous rest activity and its underlying anatomical circuitry is high were based on retrograde tracer injection studies (Vincent et al. 2007); these trace out the direct afferent connectivity of a region of interest, i.e., the injection site, but are not able to provide insight into the large scale network connectivity. Our results suggest that an anatomical connectivity analysis of the large-scale network does not suffice to identify the network constituents during rest, but rather requires an analysis of the network dynamics.

Functional connectivity analysis

To explore the network dynamics supported by the present large-scale connectivity matrix, we simulated the network dynamics computationally. We placed neuronal oscillators at each network node and initially considered multiple oscillator types which are commonly used in neural population modeling including Hopf oscillators (Breakspear and Jirsa 2007), Wilson–Cowan (Wilson and Cowan 1972) and FitzHugh–Nagumo (FitzHugh 1961; Nagumo et al. 1962) systems. Since all neural oscillators provided similar results, we present in the following the simulations based upon FitzHugh–Nagumo systems representing neural population activity (see also Assisi et al. 2005 for population modeling). Each network node was characterized by a degree of excitability, in which the increase of excitation parameterizes the onset of oscillations emerging from a quiescent state. Then the network node equations are given as

$$\dot{u}(t) = g(u,v) = \tau\left[v + \gamma u - \frac{u^3}{3}\right]$$

$$\dot{v}(t) = h(u,v) = -(1/\tau)[u - \alpha + bv - I]$$

where u and v represent the fast and slow variables respectively (Breakspear and Jirsa 2007). The network model equations are given by:

$$\dot{u}_i(t) = g(u_i, v_i) - \sum_{j=1}^{N} f_{ij} u_j\left(t - \Delta t_{ij}\right)$$

$$\dot{v}_i(t) = h(u_i, v_i)$$

where f represents the connection matrix of dimension $N \times N$ (scaled by the value 0.016 to ensure dynamic stability), N being the number of nodes and the time delays are computed from the distance matrix d and v is the propagation velocity,

$$\Delta t_{ij} = \frac{d_{ij}}{v}$$

The simulations are carried out for transient rest state dynamics i.e., there is no external stimulus, $I = 0$, and the network dynamics evolves from a random initial condition to its stable equilibrium point. This transient dynamics is typically complex and involves oscillatory behavior, which we do not characterize in more detail in the current study. Here our only concern is the measurement of the spatial network configurations activated during this transient. The parameter values are set as follows: $\alpha = 1.05$, $b = 0.2$, $\gamma = 1.0$, $\tau = 1.25$. We employed Matlab DDE23 for numerical integration. We set the propagation velocity, v, to multiple biologically realistic values and its infinite value.

To characterize the functional connectivity of this network, we apply a set of spatiotemporal measures. The first measure we apply is the integrated entropy (Tononi and Edelman 1998). Let $u(i)$ be the temporal data at ith node (in our case the fast variables from the FitzHugh–Nagumo system) and we compute the joint probability distribution $p(u(i),u(j))$ and the entropy is obtained by

$$H(i,j) = -\sum_{i=1}^{N}\sum_{j=1}^{N} p(u(i),u(j)) \log[p(u(i),u(j))].$$

Thus we obtain the entropy matrix of dimension $N \times N$, where N is the number of nodes in the connectivity matrix. To quantify the entropy contribution of each node we calculate the row or column sum (H being a symmetric matrix)

$$H(i) = \sum_{j=1}^{N} H(i,j).$$

The above quantity is known as integrated entropy, signifying statistical independence of a particular area (i) in the network from others and is shown in Fig. 2 for the velocity values ∞, 15, 7, 3, and 2 m/s. We find that for instant transmission, i.e., infinitely large velocity, the prefrontal areas (PFCORB, PFCCL) show higher integrated entropy compared to the rest of the nodes while for finite velocities there emerge links to anterior cingulate (CCA) and other areas, in particular also to CCP

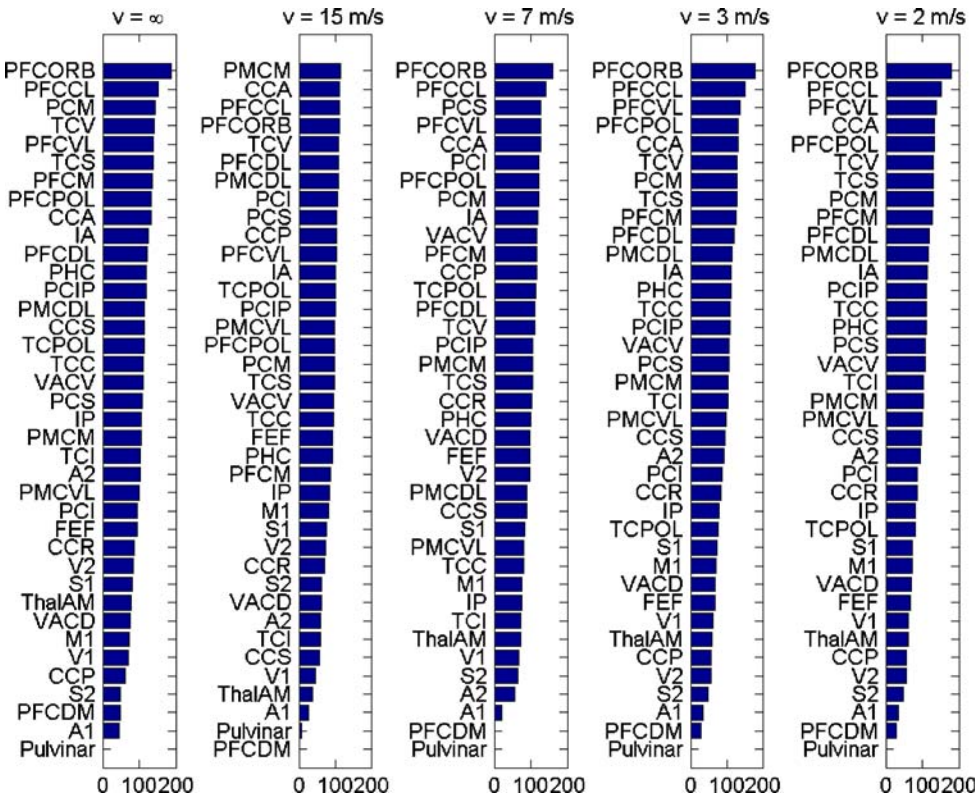

Fig. 2 Integrated entropy for transmission speeds ∞, 15, 7, 3, and 2 m/s

at 7 and 15 m/s. This is indicative of the feature that in the resting state of brain there is an underlying cingulate–prefrontal sub network. However, the above result shows, rather weakly, this cingulate–prefrontal connection. We extend the analysis of the spatiotemporal data in wavelet domain and will discuss the method and results in the following section.

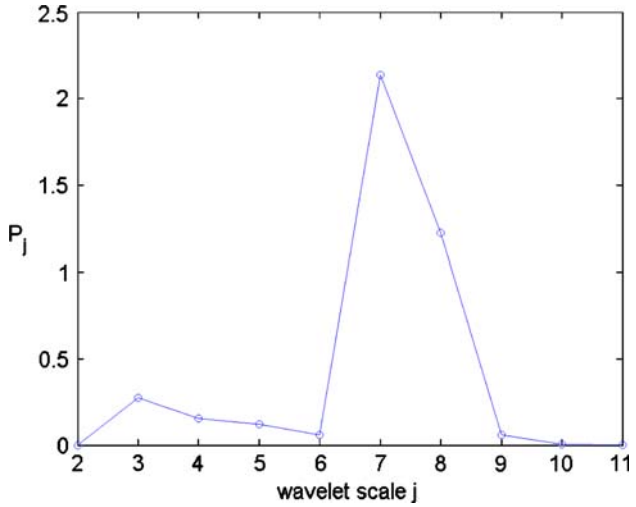

Fig. 3 Averaged wavelet power spectrum

Wavelet transform decomposes a signal into both time and scale (equivalently frequency) and has been widely used to analyze experimental EEG and fMRI data (Salvador et al. 2007). The main advantage of wavelets over traditional Fourier analysis is that they are applicable to non-stationary signals as often encountered in experimental neuroscience data. Wavelets are sets of compact orthonormal functions, ψ_{jk}, constructed by means of dyadic translations and dilations

$$\psi_{jk}(x) = 2^{j/2}\psi(2^j x - k)$$

where integers j,k indicate dilation and translation index, respectively and discrete wavelet transform of signal $x(n)$ is given by

$$W_{jk} = \sum_n x(n)\psi_{jk}(n)$$

There exists a large family of wavelet functions, and in our analysis we have used Haar and Daubechies family of wavelets (Daubechies 1992). We take the wavelet transform of the temporal data at each node and obtain the wavelet coefficients W. The average wavelet power spectrum (averaged over all nodes) shows a maximum in power corresponding to wavelet scale $j = 7 = j_{\mathrm{m}}$ (Fig. 3).

We compute the covariance matrix, C, from the wavelet coefficients corresponding to scale $j = j_{\mathrm{m}}$, for nodes say, p and q, which is given by

Fig. 4 The functional connectivity obtained from wavelet covariance matrix

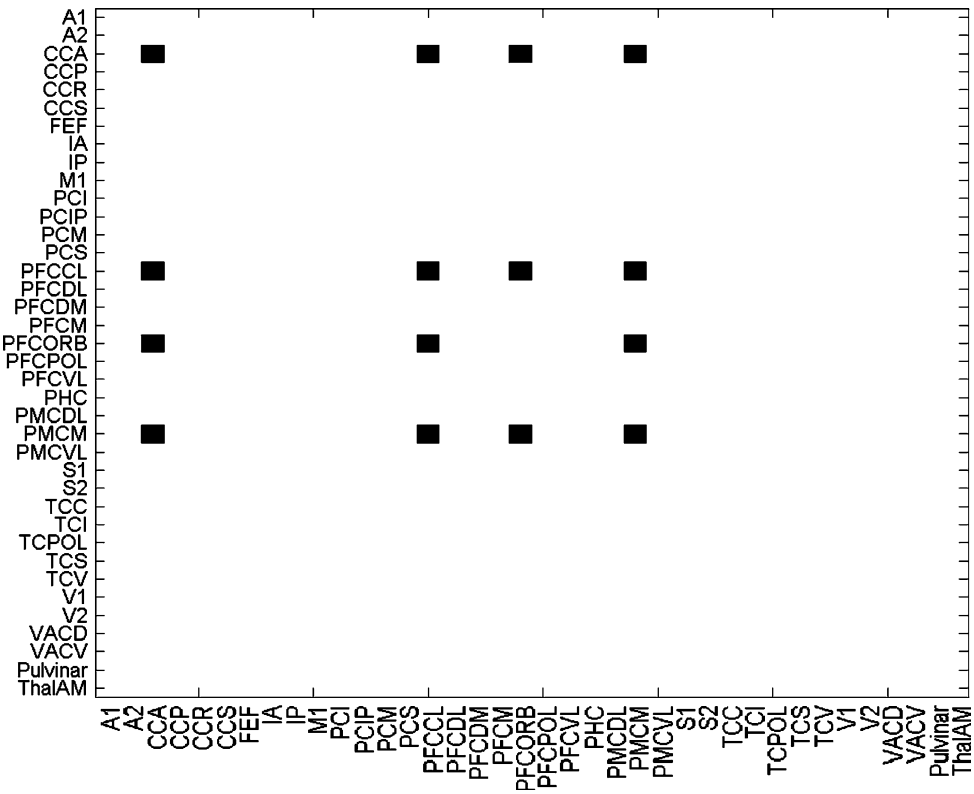

$$C_{p,q} = Cov(W^p_{jm}, W^q_{jm})$$

In Fig. 4 we show the thresholded covariance matrix, where the threshold has been chosen as $c_{\text{th}} = 0.15$ and dark spots have strength greater than c_{th}. The threshold is chosen such that entries in the connectivity matrix lie outside the standard deviation calculated for all elements in the covariance matrix, C. The covariance matrix clearly indicates that the functional subnetwork in resting state is cingulate–prefrontal and medial premotor in nature. Similar analysis for low velocities yield only a single dominating entry namely PFCORB, indicating the other areas are implicated for higher velocity regimes.

Conclusions

For increasing transmission speed the sub-networks present in transient rest state activity disengage the cingulate components and are left with only its prefrontal contributions for instantaneous transmission, thus resembling characteristics of anatomical connectivity. Hence we find evidence that the introduction of time delays aids in the additional recruitment of cingulate cortex. This suggests that the space–time structure of the time delays is crucial for the understanding of the brain's rest state. In fact, our results demonstrate that the correlation structure of the rest state networks previously observed in experiments can be understood on the basis of the spatial (anatomical connectivity) and temporal (time delays) properties of connectivity. Our findings are consistent with the proposal that coherent spontaneous fluctuations of the resting brain reflect a more fundamental or intrinsic property of functional organization of the human brain (Jirsa 2004); not exclusively dependent on the presence of conscious mental activity.

Acknowledgements RK acknowledges support by the Deutsche Forschungsgemeinschaft and VKJ acknowledges support by the ATIP (Centre National de la Recherche Scientifique). ARM, RK and VKJ were supported by the JS McDonnell Foundation.

Appendix: list of cortical areas

A1	Primary auditory
A2	Secondary auditory
CCA	Anterior cingulate cortex
CCP	Posterior cingulate cortex
CCR	Retrosplenial cingulate cortex
CCS	Subgenual cingulate cortex
FEF	Frontal eye field
IA	Anterior insula
IP	Posterior insula
M1	Primary motor cortex
PCI	Inferior parietal cortex
PCIP	Intraparietal sulcus cortex
PCM	Medial parietal cortex
PCS	Superior parietal cortex
PFCCL	Centrolateral prefrontal cortex
PFCDL	Dorsolateral prefrontal cortex
PFCDM	Dorsomedial prefrontal cortex
PFCM	Medial prefrontal cortex
PFCORB	Orbital prefrontal cortex
PFCPOL	Prefrontal polar cortex
PFCVL	Ventrolateral prefrontal cortex
PHC	Parahippocampal cortex
PMCDL	Dorsolateral premotor cortex
PMCM	Medial (supplementary) premotor cortex
PMCVL	Ventrolateral premotor cortex
S1	Primary somatosensory cortex
S2	Secondary somatosensory cortex
TCC	Central temporal cortex
TCI	Inferior temporal cortex
TCPOL	Polar temporal cortex
TCS	Superior temporal cortex
TCV	Ventral temporal cortex
V1	Primary visual cortex
V2	Secondary visual cortex
VACD	Dorsal anterior visual cortex
VACV	Ventral anterior visual cortex
Pulvinar	Pulvinar
ThalAM	Anteromedial thalamus

References

Assisi CG, Jirsa VK, Kelso JAS (2005) Synchrony and clustering in heterogeneous networks with global coupling and parameter dispersion. PRL 94:018106

Bar M (2007) The proactive brain: using analogies and associations to generate predictions. Trends Cogn Sci 11(7):280–289

Biswal B, Yetkin FZ, Haughton VM, Hyde JS (1995) Functional connectivity in the motor cortex of resting human brain using echo-planar MRI. Magn Reson Med 34:537–541

Breakspear M, Jirsa VK (2007) Neuronal dynamics and brain connectivity. In: Jirsa VK, McIntosh ARM (eds) Handbook of brain connectivity. Springer

Damoiseaux JS et al (2006) Consistent resting-state networks across healthy subjects. Proc Natl Acad Sci USA 103:13848–13853

Daubechies I (1992) Ten lectures on wavelets. SIAM

FitzHugh R (1961) Impulses and physiological states in theoretical models of nerve membrane. Biophys J 1:445–466

Fox MD et al (2005) The human brain is intrinsically organized into dynamic, anticorrelated functional networks. Proc Natl Acad Sci USA 102:9673–9678

Greicius MD, Krasnow B, Reiss AL, Menon V (2003) Functional connectivity in the resting brain: a network analysis of the default mode hypothesis. Proc Natl Acad Sci USA 100:253–258

Gusnard DA, Raichle ME (2001) Searching for a baseline: Functional imaging and the resting human brain. Nat Rev Neurosci 2:685–694

Honey CJ, Kötter R, Breakspear M, Sporns O (2007) Network structure of cerebral cortex shapes function connectivity on multiple time scales. Proc Natl Acad Sci USA 104:10240–10245

Jirsa VK (2004) Connectivity and dynamics of neural information processing. Neuroinformatics 2(2):183–204

Kötter R (2004) Online retrieval, processing, and visualization of primate connectivity data from the CoCoMac database. Neuroinformatics 2:127–144

Kötter R (2005) Wanke Mapping brains without coordinates. Philos Trans R Soc Lond B 360:751–766

Nagumo J, Arimoto S, Yoshizawa S (1962) An active pulse transmission line simulating nerve axon. Proc IRE 50:2061–2070

Salvador R, Achard S, Bullmore ET (2007) Frequency dependent functional connectivity analysis of fMRI data in Fourier and wavelet domains. In: Jirsa VK, McIntosh ARM (eds) Handbook of brain connectivity. Springer

Tononi G, Edelman GM (1998) Consciousness and complexity. Science 282:1846–1851

Vincent JL et al (2006) Coherent spontaneous activity identifies a hippocampal-parietal memory network. J Neurophysiol 96:3517–3531

Vincent JL, Patel GH, Fox MD, Snyder AZ, Baker JT, Van Essen DC, Zempel JM, Snyder LH, Corbetta M, Raichle ME (2007) Intrinsic functional architecture in the anaesthetized monkey brain. Nature 447:83–86

Wilson HR, Cowan JD (1972) Excitatory and inhibitory interactions in localized populations of model neurons. Biophys J 12:1–23